a

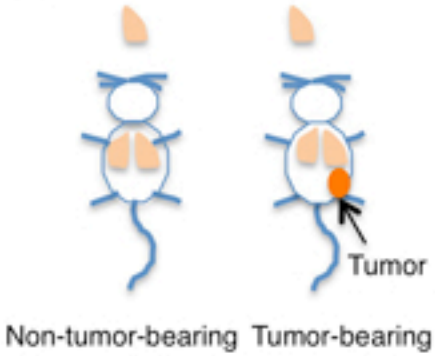

	Receptor name	Accession number	Fold change
Fcgr2b	beta Fc receptor type II (FCRII)CD32	M31312	6.3
Ccr2	mcp-1 receptor	U56819	5.7
Il1r2 CD121b	Il-1r2 mRNA for type II interleukin-1 receptor	X59769	4.4
Gpr65	putative G protein-coupled receptor TDAG8 (TDAG8)	U39827	4.3
Lilra6	immunoglobulin-like receptor PIRA3 (7M1)	U96684	4.2
Ccr1	chemokine G-protein-coupled receptor CCR-1	U29678	4.1
Pira1	immunoglobulin-like receptor PIRA1 (6M21)	U96682	3.3
Csf3r	granulocyte colony-stimulating factor receptor	M58288	3

b

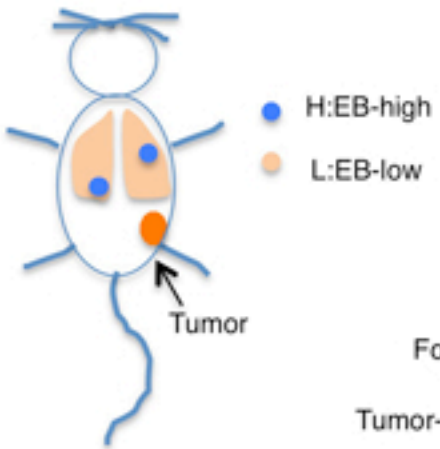

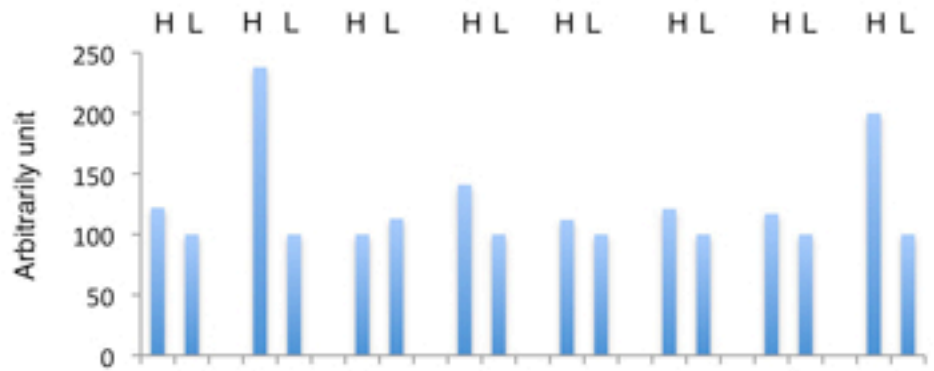

Fold change	*Fcgr2b*	*Ccr2*	*Il1r2*	*Gpr65*	*Lilra6*	*Ccr1*	*Pira1*	*Csf3r*
Tumor-/Non-tumor-bearing X EB-high/EB-low area in tumor-bearing	6.3	5.7	4.4	4.3	4.2	4.1	3.3	3
	1.2	2.3	0.9	1.4	1.1	1.2	1.1	2
EB-high in tumor-bearing/ Non-tumor-bearing	7.6	13.1	4	6	4.6	4.9	3.6	6

Supplementary Figure S1. A list of the receptors which were significantly up-regulated in LLC-bearing mouse lungs. **a**. A comparison of the gene expression level between tumor-bearing- and non-tumor-bearing- mouse lungs shown as fold changes (brown). **b**, The fold changes of mRNA levels in regions between Evans Blue (EB)-high leakage and EB-low leakage in tumor-bearing mouse lungs (numbers shown as green). *CCR2* showed the highest value in the ratio of EB-high area in tumor-bearing over EB-low area in normal mouse lungs (numbers shown as red).

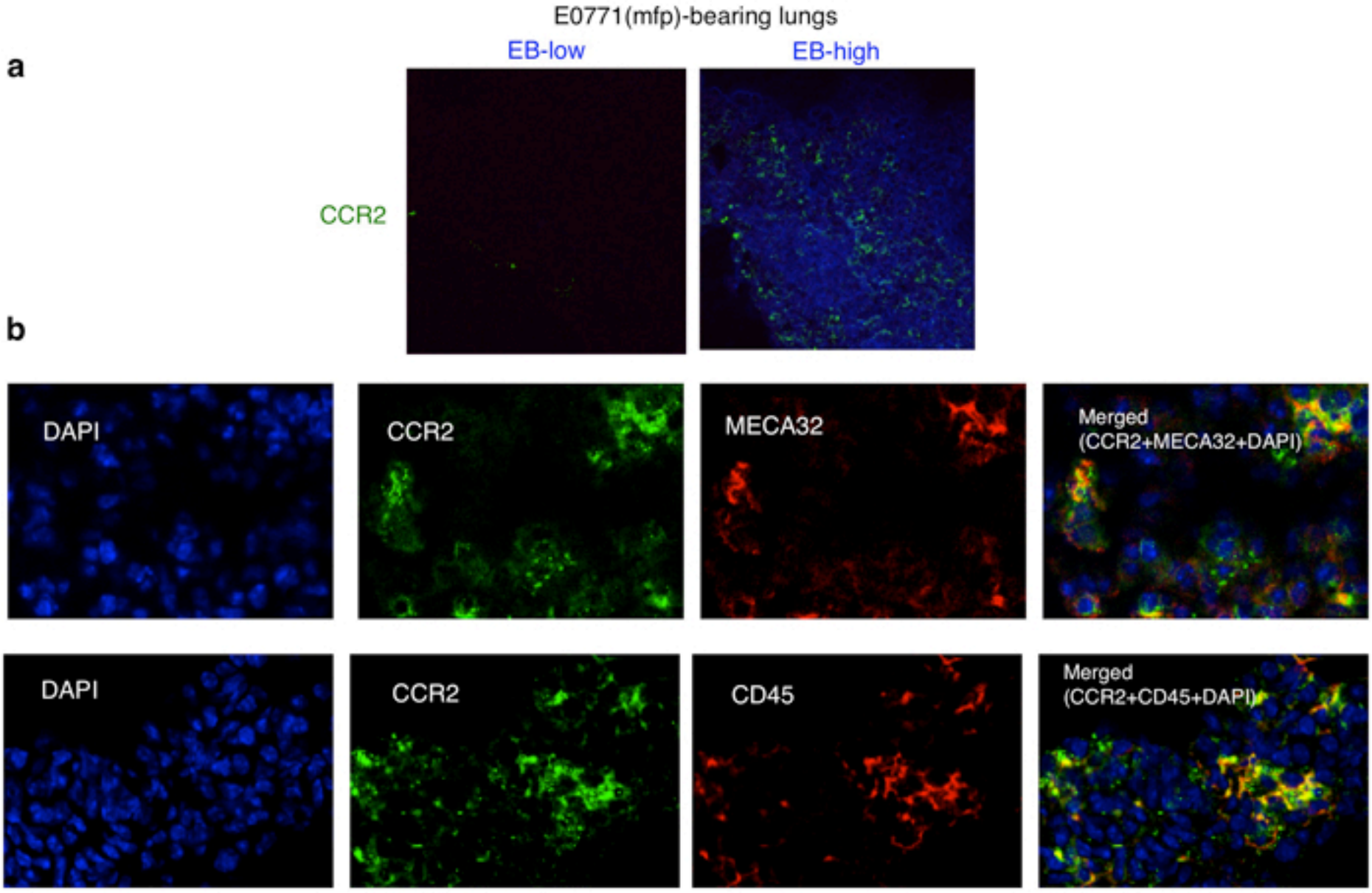

Supplementary Figure S2. a, Immunohistochemical detection of CCR2 expression (green) in Evans blue (EB)-high leakage region and EB-low leakage region of E0771-mammaly fat pad (mfp)-bearing mouse lungs. EB was detected at Cy5 channel (blue). **b**, MECA32 and CD45 expression in $CCR2^{+}$-cells.

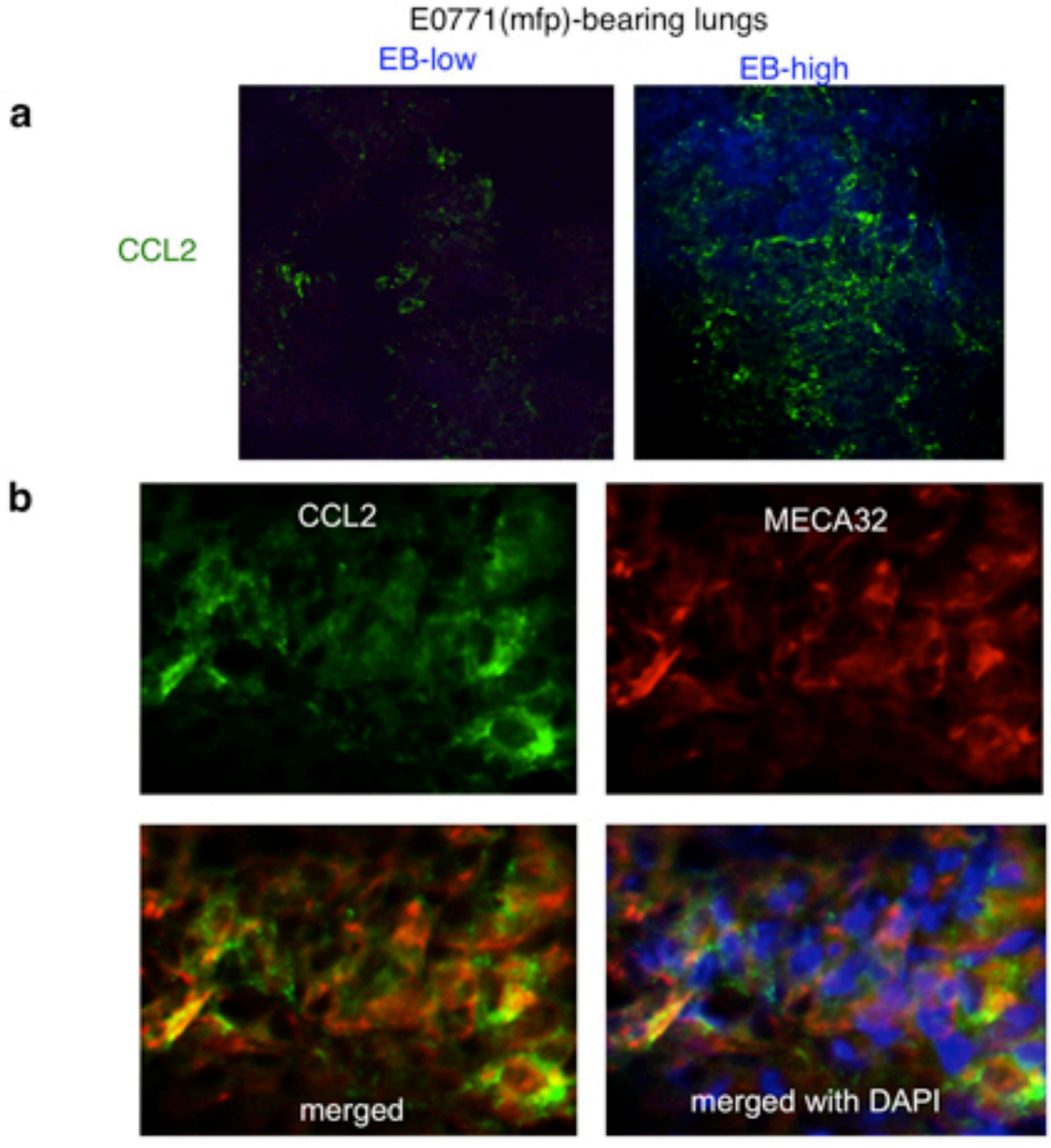

Supplementary Figure S3. a, Immunohistochemical detection of CCL2 expression (green) in Evans blue (EB)-high leakage region and EB-low leakage region of E0771-mammaly fat pad (mfp)-bearing mouse lungs. **b**, MECA32 expression in CCL2^{+}-cells.

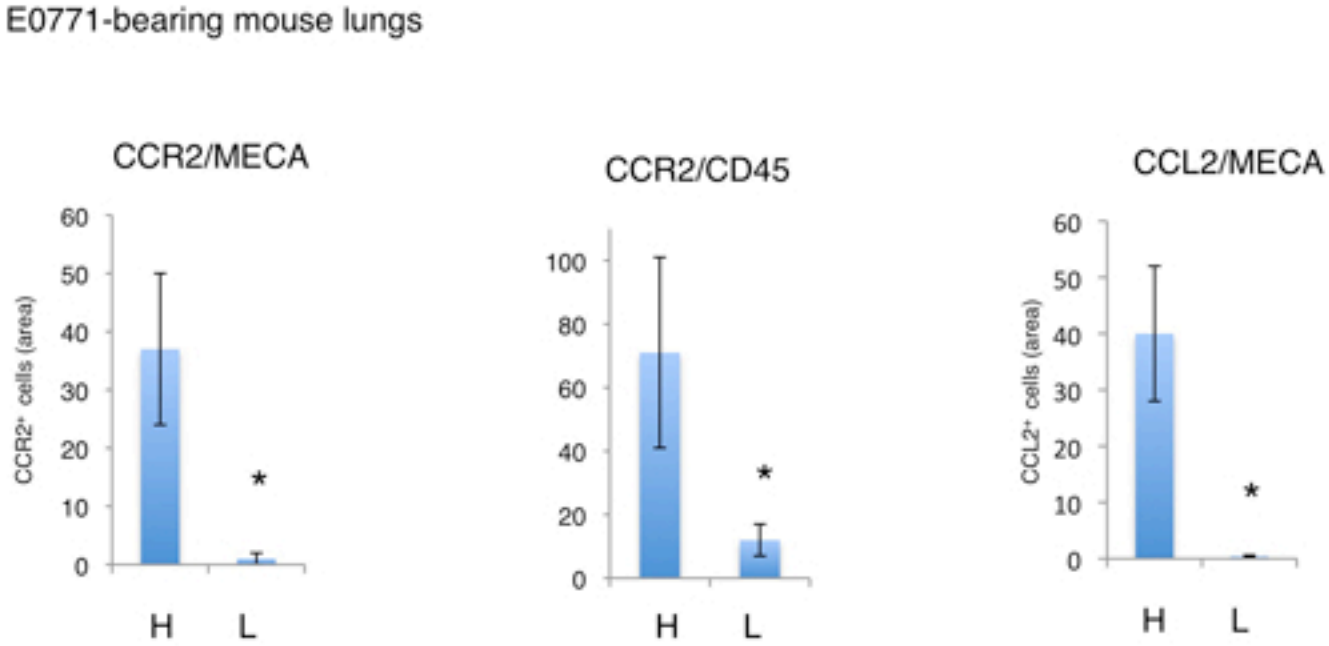

Supplementary Figure S4. Immunohistochemical quantification of CCL2 and CCR2 expression in an endothelial marker and leukocyte common antigen, MECA32-positive and CD45-positive cells respectively in the high-leakage area (H) or low-leakage area (L) of E0771-bearing mouse lungs. *, $P<0.05$.

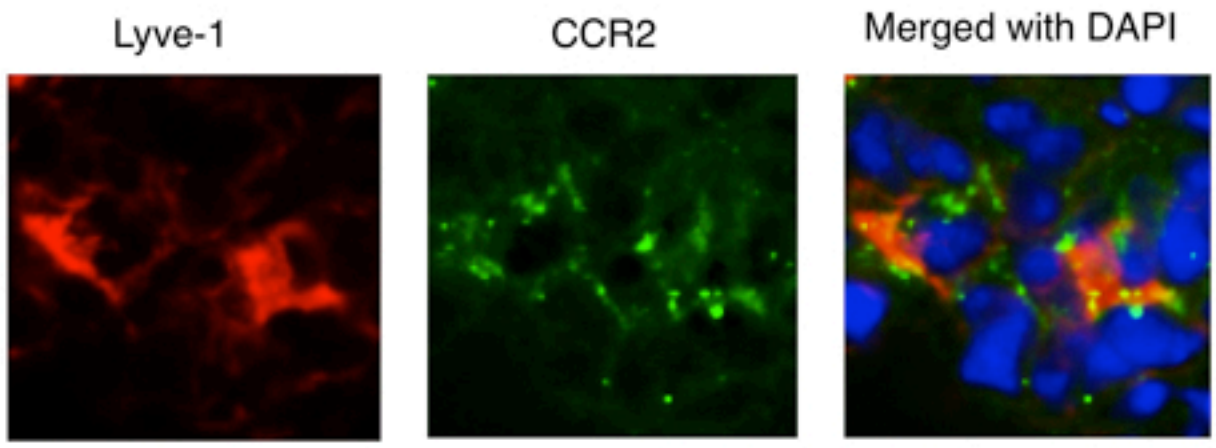

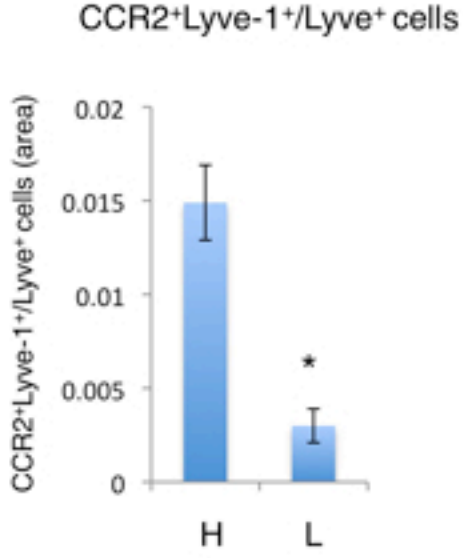

Supplementary Figure S5. Lyve-1$^+$/CCR2$^+$ cells (~1.5% among Lyve-1+ cells) in hyperpermeable regions (H) in E0771-bearing mouse lungs. n=6. P=0.0009

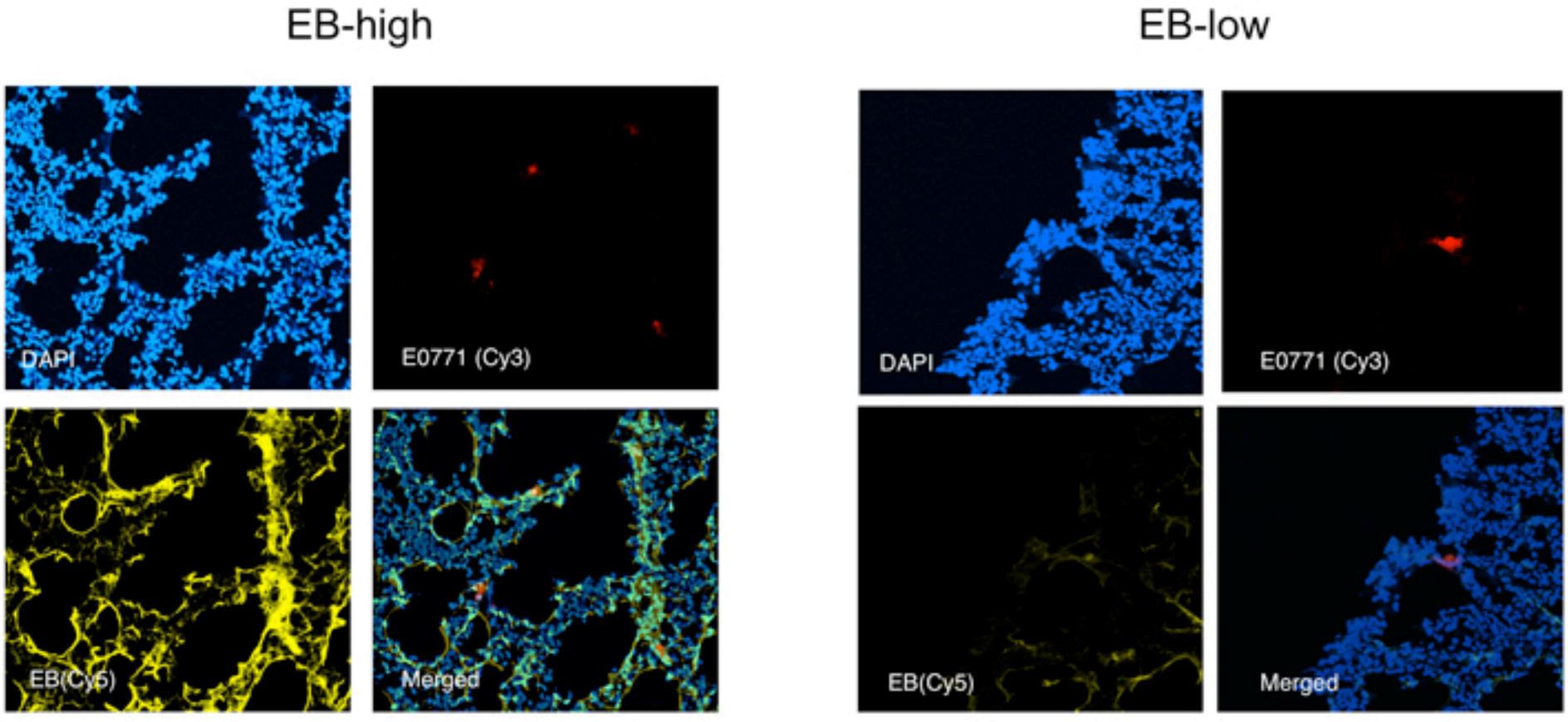

Supplementary Figure S6. Increase of rhodamine-labeled E0771 in hyperpermeable (EB-high) regions in E0771-bearing mouse lungs

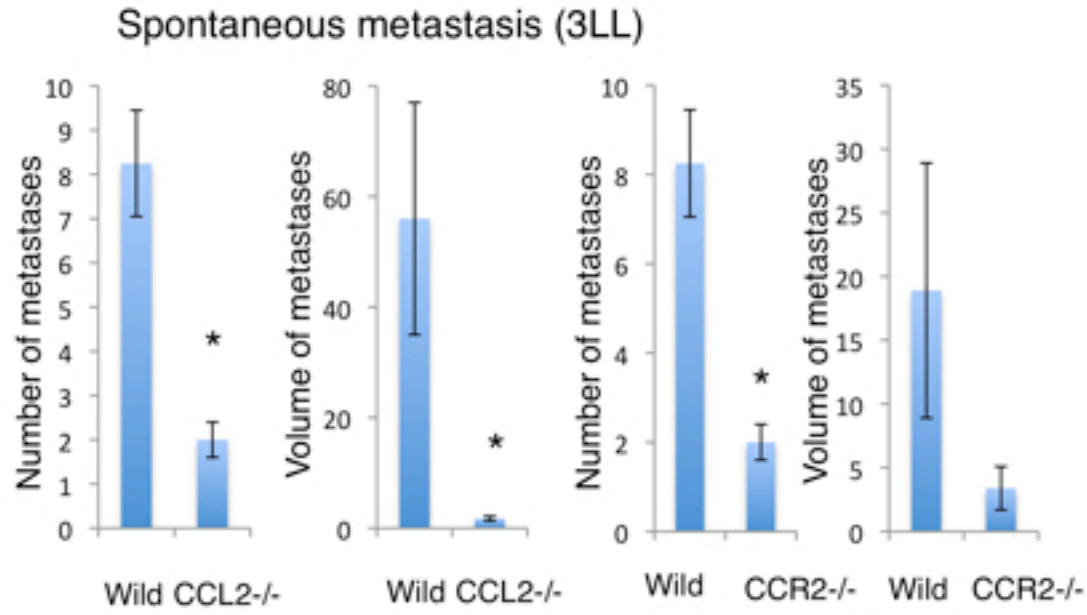

Supplementary Figure S7. The number and volume of metastatic nodules in wild-type, CCL2-/- or CCR2-/- mouse lungs 3 weeks after subcutaneous injection of highly metastatic Lewis lung carcinoma (3LL). n=4. *, P<0.05.

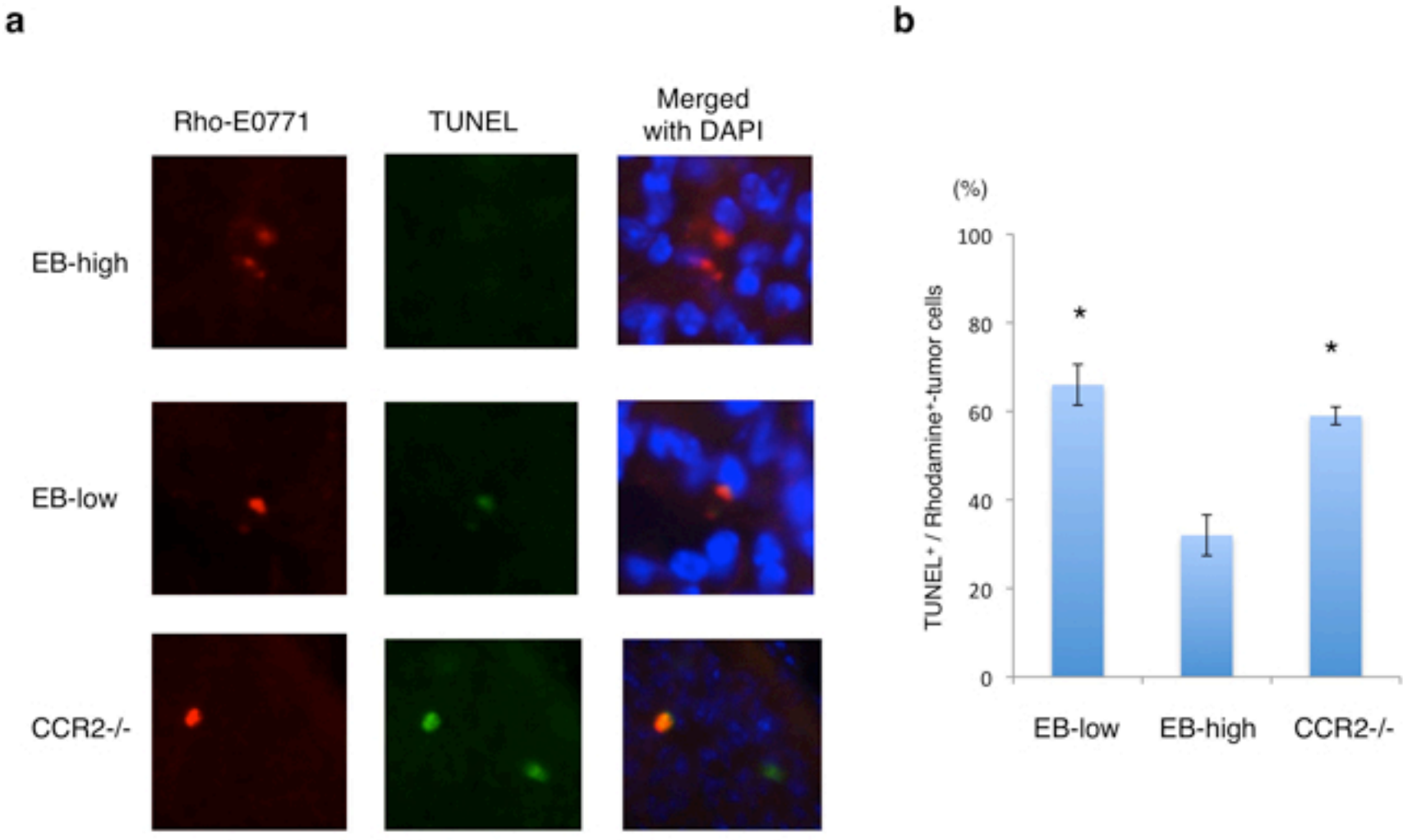

Supplementary Figure S8. Tumor cells show TUNEL signals in EB-low and EB-high area in E0771-bearing wild-type or CCR2-/- mouse lungs 72hrs after E0771 cell injection. **a**, Immunohistochemical detection of TUNEL signals (green) in rhodamine-labeled E0771 cells (red). **b**, Immunohistochemical quantification of TUNEL$^+$/rhodamine$^+$ cells. n=7. P=0.006

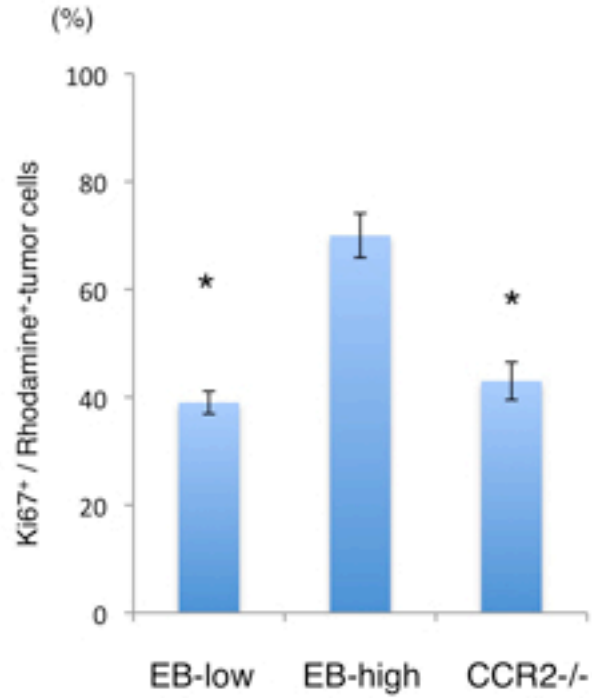

Supplementary Figure S9. Tumor cells show Ki67 signals in EB-low and EB-high area in E0771-bearing wild-type or CCR2-/- mouse lungs 72hrs after E0771 cell injection. Immunohistochemical quantification of $Ki67^{+}$/$rhodamine^{+}$ cells. n=7. P=0.002 (EB-low vs EB-high) and P=0.007 (EB-high vs CCR2-/-)

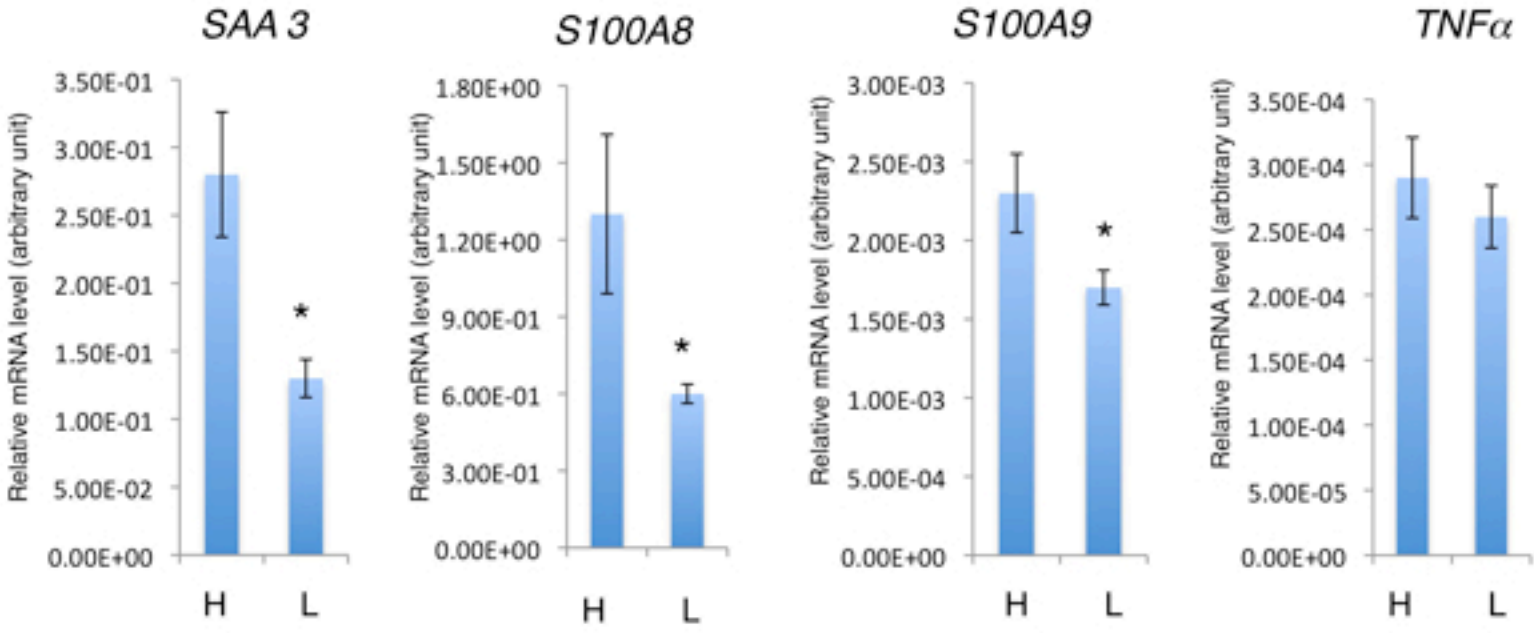

Supplementary Figure S10. The different expression of *SAA3, S100A8, S100A9* and *TNFα* between high- and low- permeable regions in E0771-bearing mouse lungs. The mRNA levels were detected by quantitative PCR and normalized by β-actin. *, $P<0.05$.

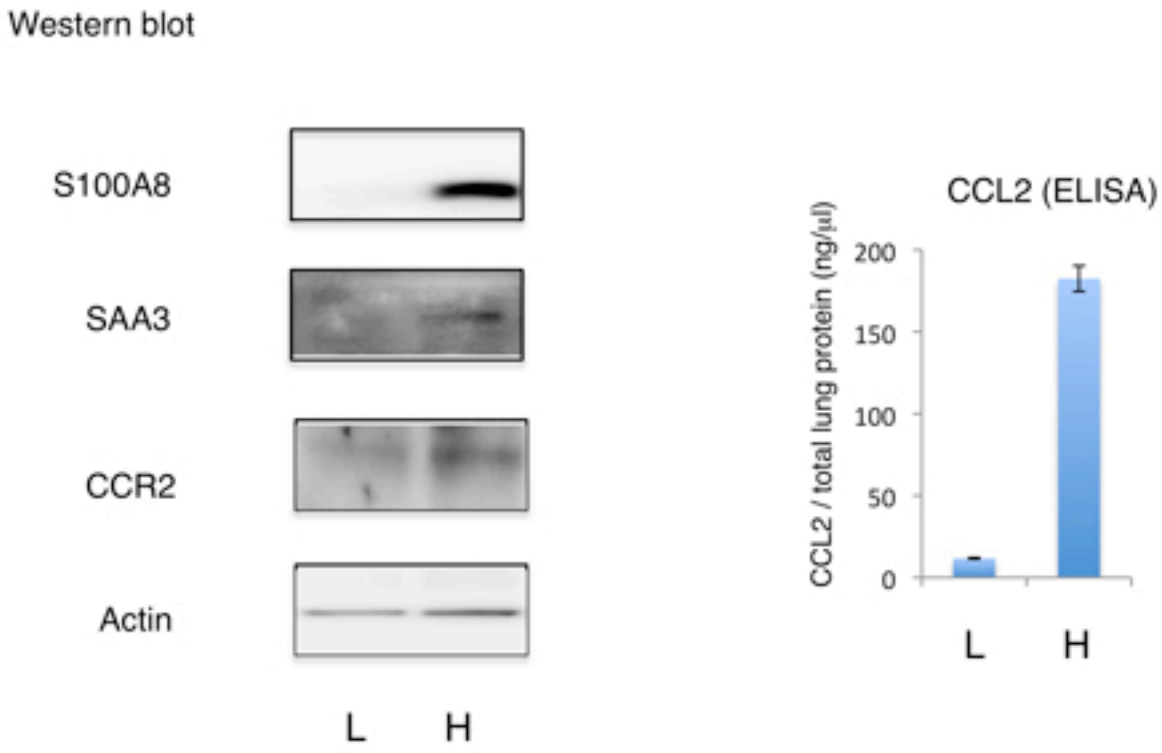

Supplementary Figure S11. Increased expression of S100A8, SAA3, CCR2 and CCL2 proteins in hyperpermeable (H) region

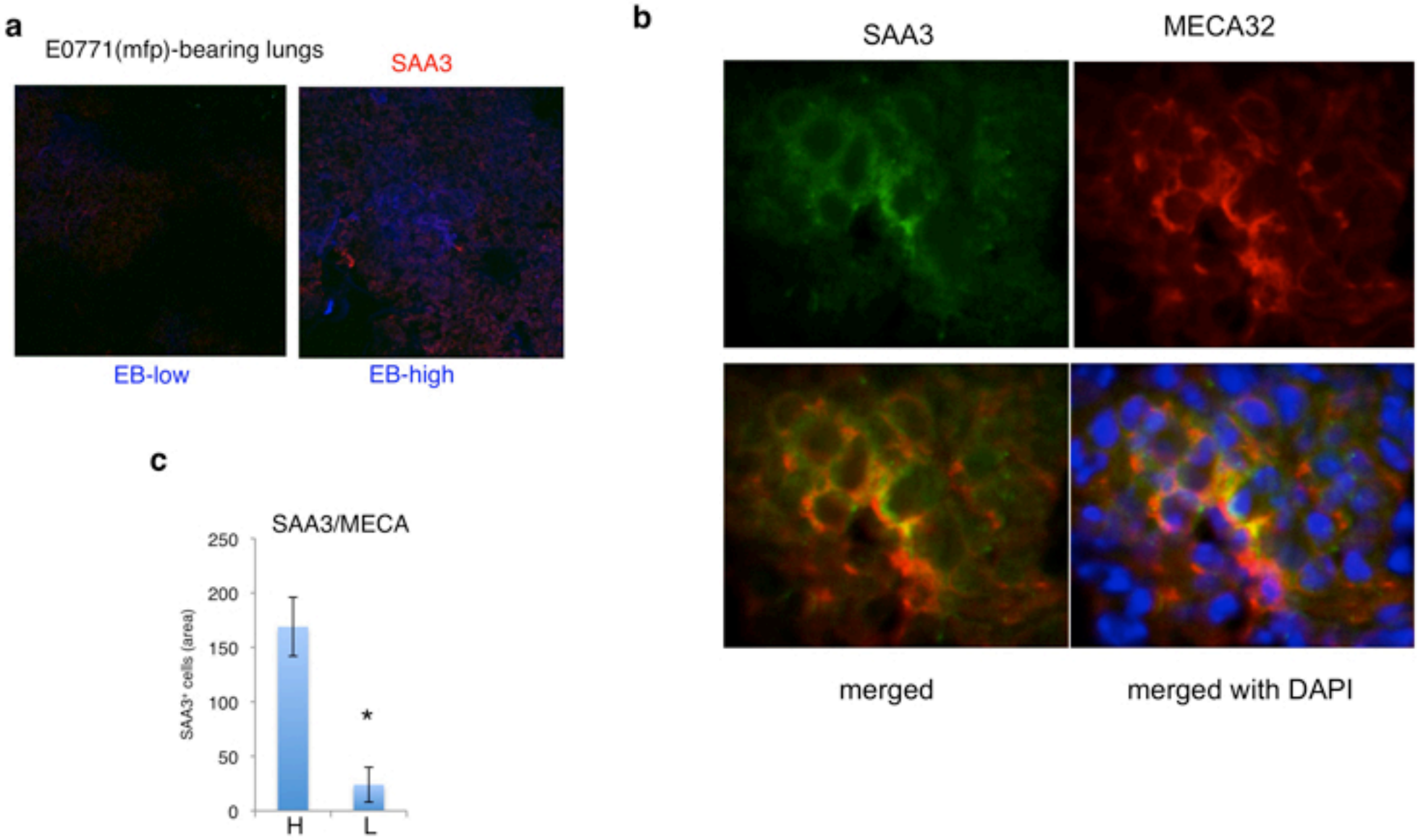

Supplementary Figure S12. a. Immunohistochemical staining of SAA3 proteins (red) in EB-high leakage region and EB-low leakage region of E0771-bearing mouse lungs. EB leakage was evidenced by blue signal. **b,** SAA3 (green) induction in MECA32^{+}-endothelial cells(red) in EB-high regions. **c**. The quantitative difference of SAA3 expression in endothelial cells between the high- (H) and low- (L) leakage regions in E0771-bearing mice. *, $P<0.05$.

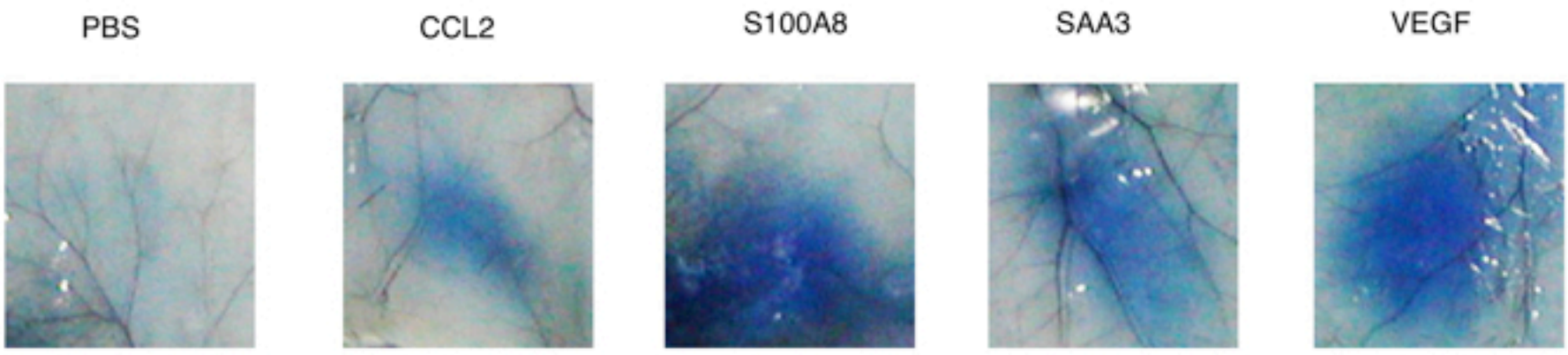

Supplementary Figure S13. Miles assay: representative permeability data in wild-type mouse 15 min after application of PBS, CCL2, S100A8, SAA3 or VEGF in the skin followed by EB intravenous injection.

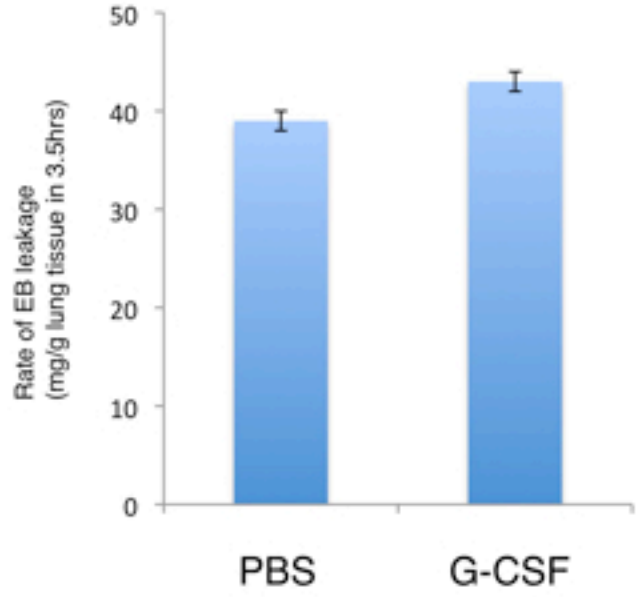

Supplementary Figure S14. G-CSF-mediating lung permeability. EB-leakage was measured 3.5 after EB injection. n=6.

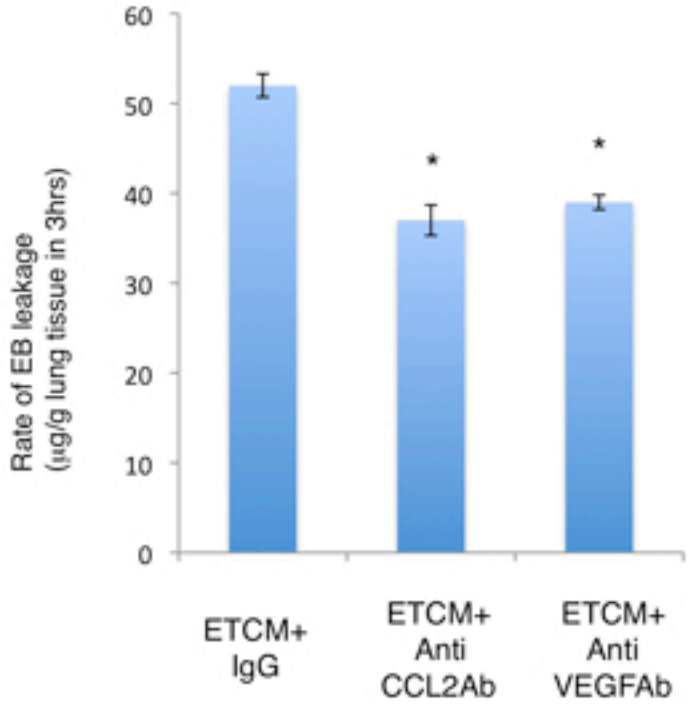

Supplementary Figure S15. Neutralizing anti-CCL2 antibody suppressed TCM-mediating lung permeability as same level as that by an anti-VEGF antibody. n=6
*P<0.05

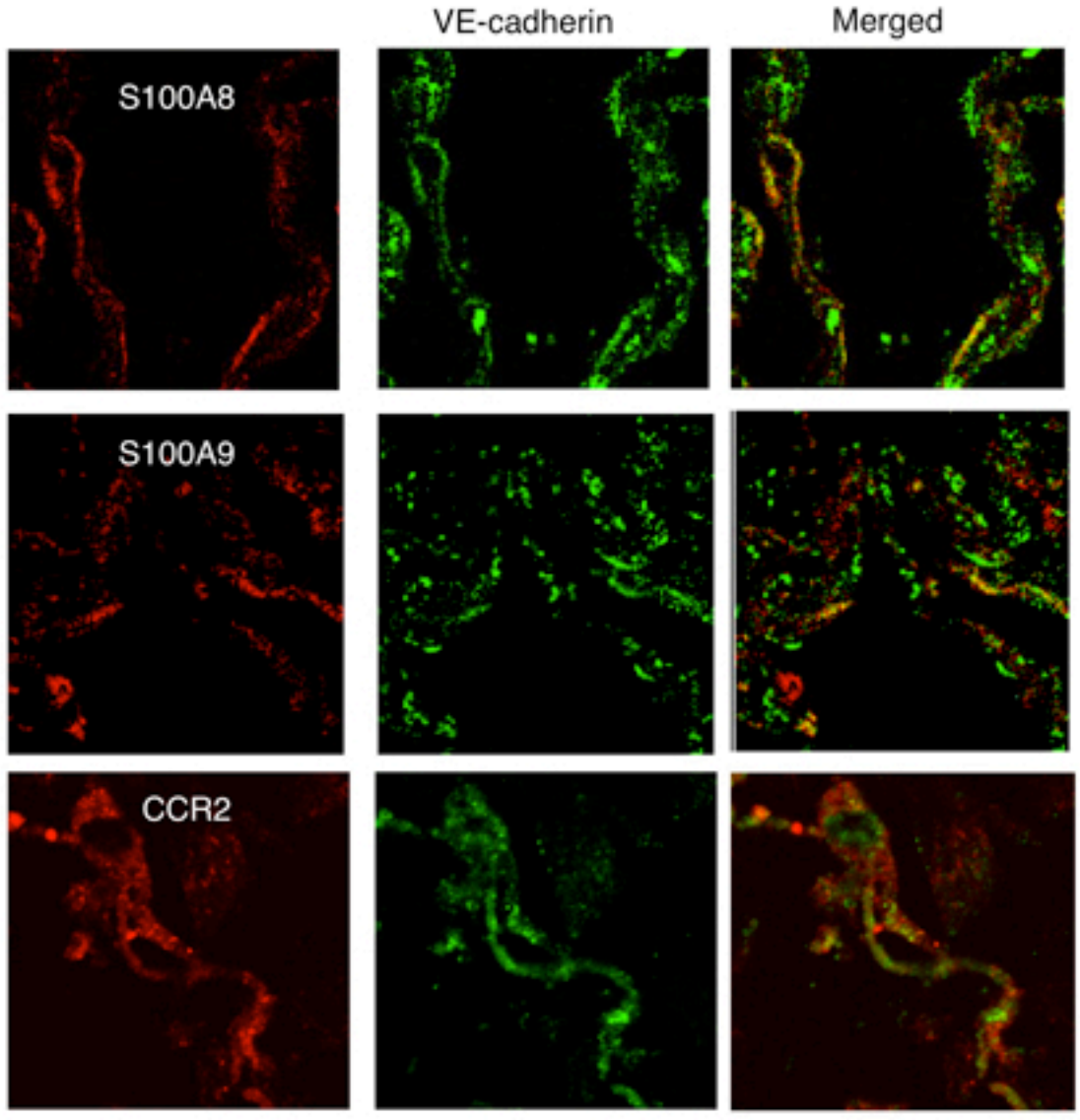

Supplementary Figure S16. Immunostaining of S100A8, S100A9 and CCR2 expression in VE-cadherin^{+}-endothelial cells in tumor-bearing human lungs

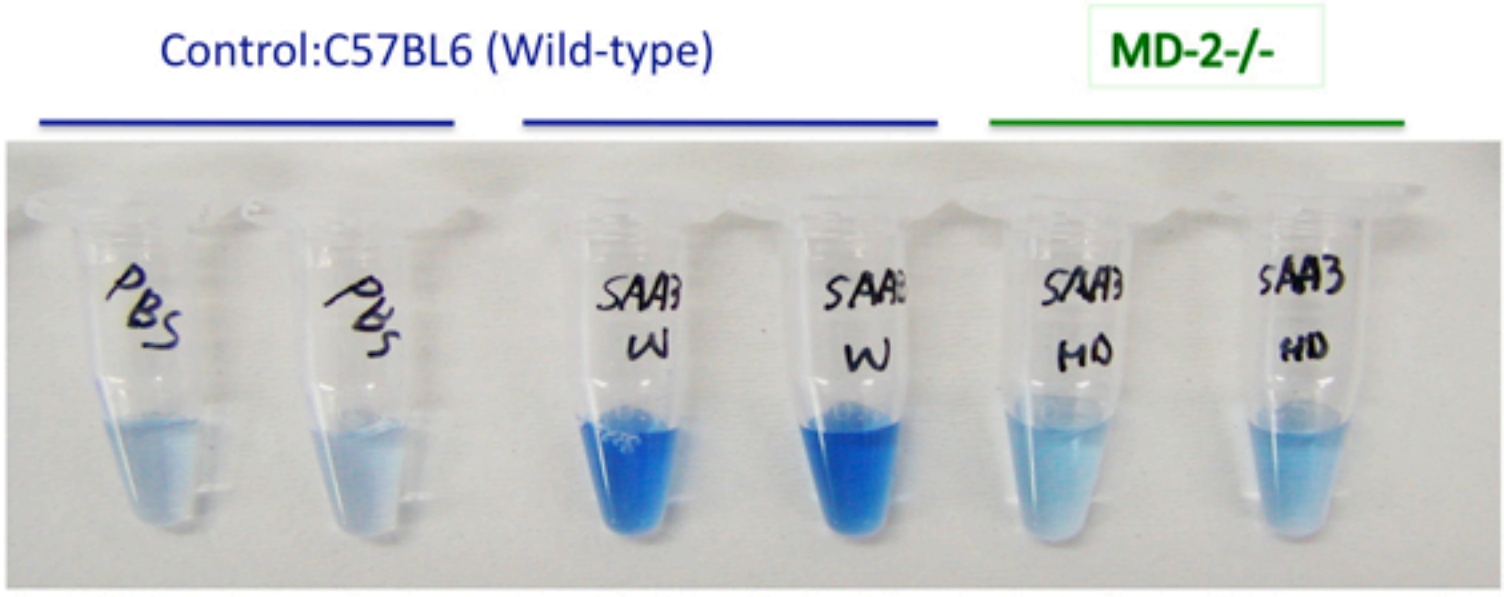

Supplementary Figure S17. Representative photographs of peritoneal leakage induced by murine SAA3 protein derived from mammalian cells in wild-type and MD-2-/- mice.

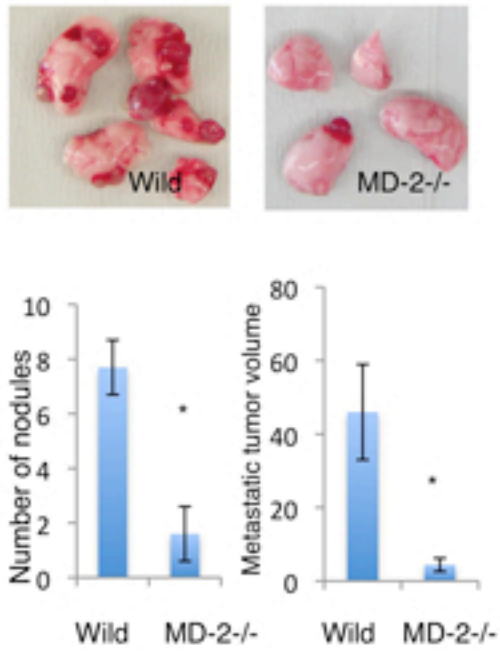

Supplementary Figure S18. Suppression of 3LL spontaneous lung metastases in MD-2-/- mice (n=5-7) .

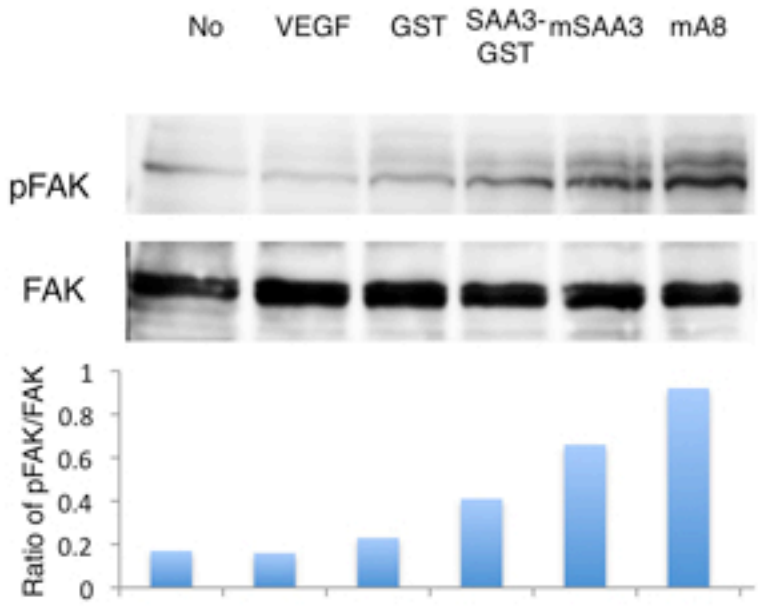

Supplementary Figure S19. Western blot showing phosphorylation of FAK (pFAK) and total FAK in murine TLR4/MD-2-overexpressing BaF cells stimulated with VEGF, SAA3 or S100A8 (A8). Both SAA3-GST (from E. Coli) and mSAA3 (from mammalian 293 cells) proteins with polymyxin B activated pFAK (upper panel). The intensity of the band of pFAK was normalized with total FAK (lower panel).

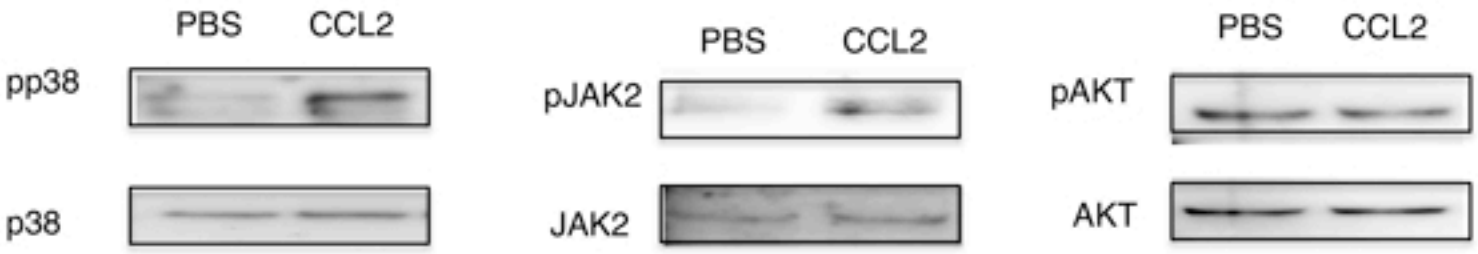

Supplementary Figure S20. CCL2 induced phosphorylation of p38 and JAK2 in CD31^{+}/CD102^{+}- lung endothelial cells. Western blot analysis for phosphorylation of p38, JAK2 and AKT.

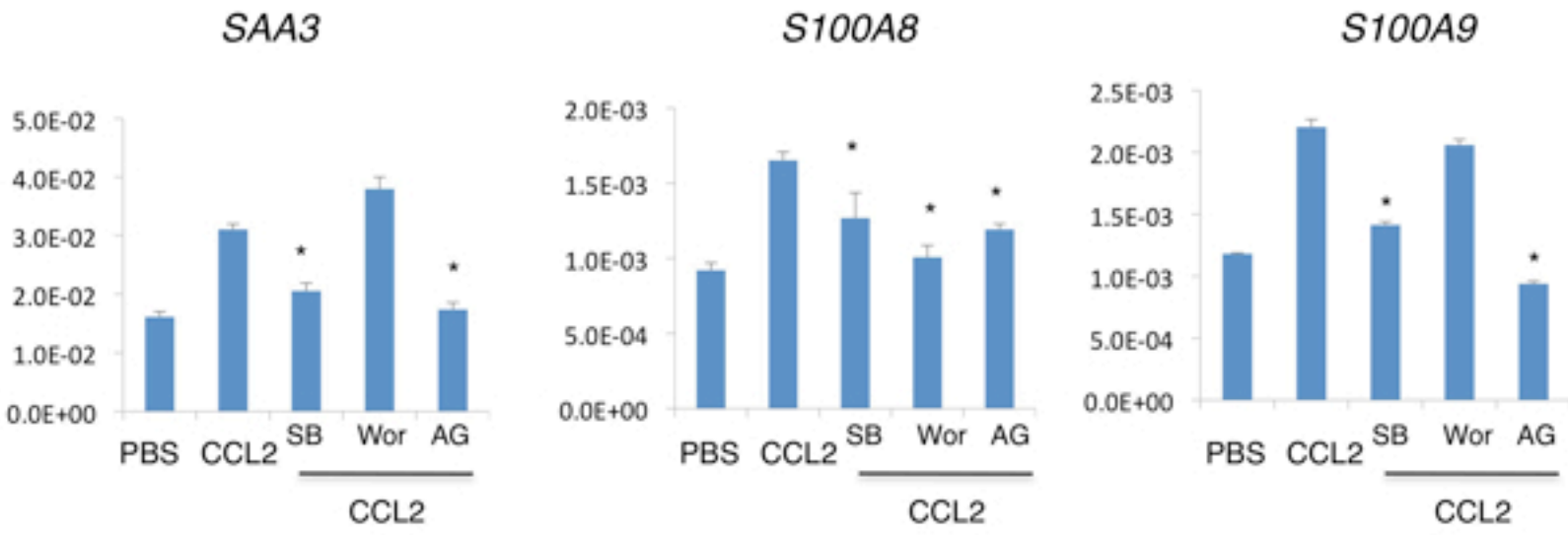

Supplementary Figure S21. *SAA3*, *S100A8* and *S100A9* expression via CCL2 signal cascade in lung endothelial ($CD31^+/CD102^+$) cells. SB203580 (2μM), Wortmannin (1μM) and AG490 (8μM) were used as inhibitors. The mRNA levels were detected by quantitative PCR and normalized by β-actin. n=3. *$P<0.05$.

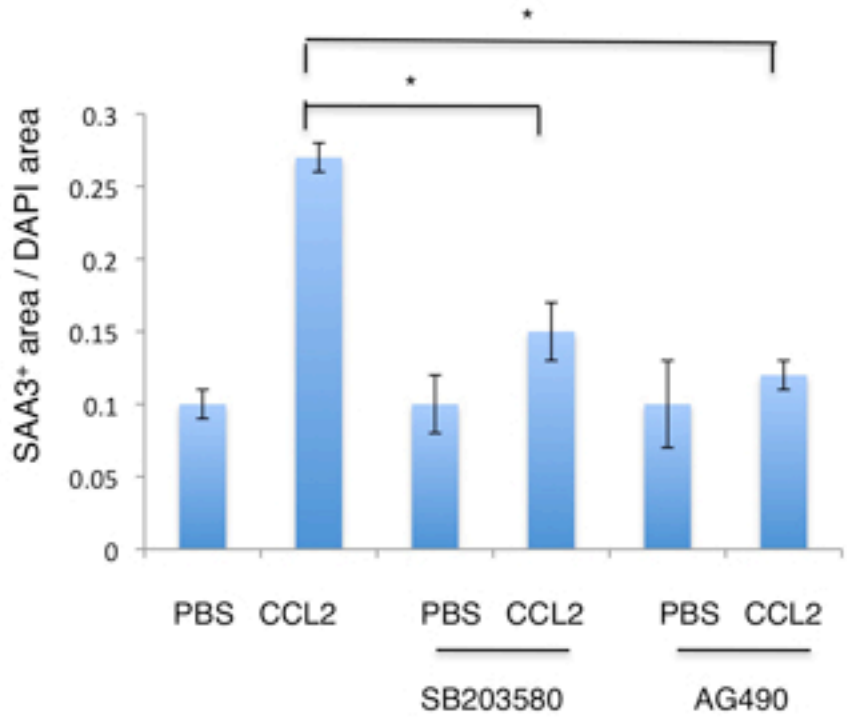

Supplementary Figure S22. Immunohistochemical quantification of SAA3 protein expression via CCL2 signal cascade in lung endothelial ($CD31^+/CD102^+$) cells. SB203580 or AG490 inhibited CCL2(100ng/ml)-mediated SAA3 expression. n=4-5. $P<0.05$.

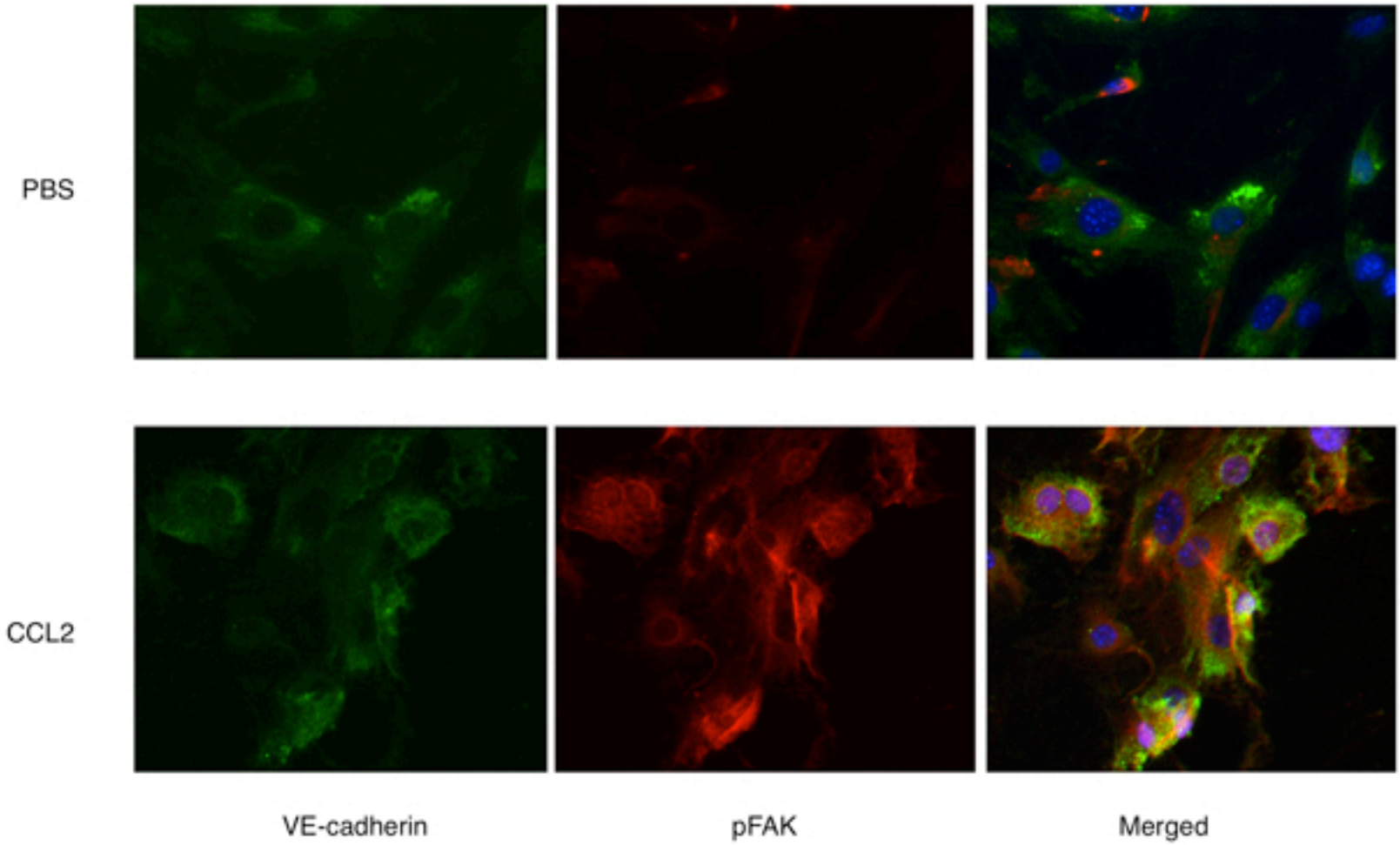

Supplementary Figure S23. Immunohistochemical detection of FAK phosphorylation by CCL2 in lung endothelial cells CD31- and CD102-double positive endothelial cells expressed an endothelial specific marker, VE-cadherin.

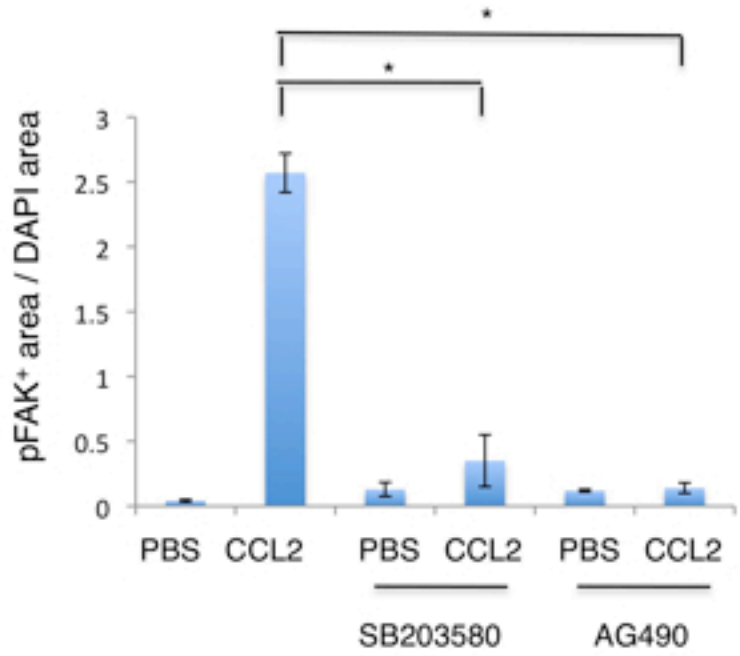

Supplementary Figure S24. Immunohistochemical quantification of FAK phosphorylation signals via CCL2 signal cascade in lung endothelial ($CD31^+/CD102^+$) cells. SB203580 or AG490 suppressed CCL2-mediated pFAK induction.
n=4-5. $P<0.05$.

Supplementary Figure S25. Full-sized western blots.

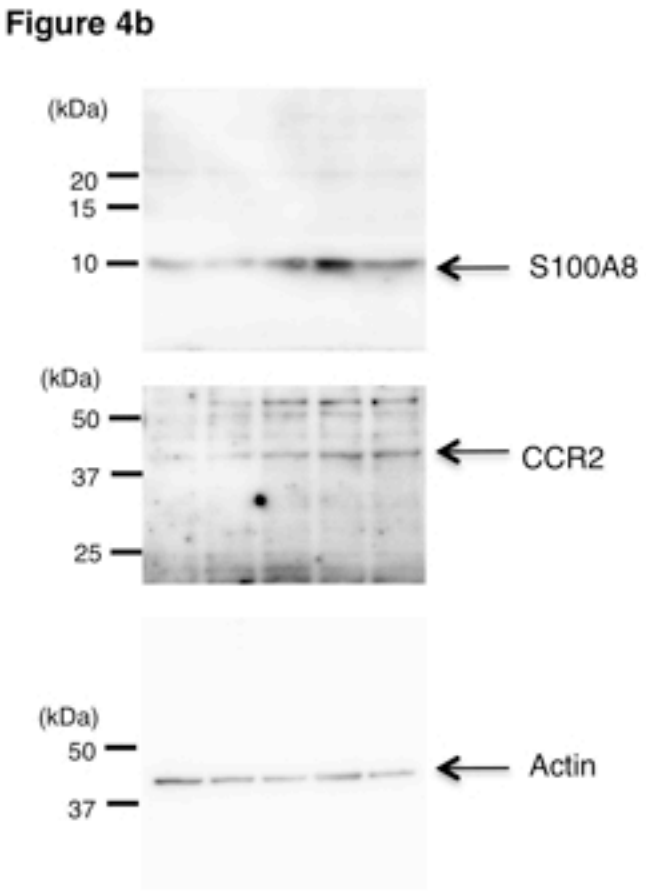

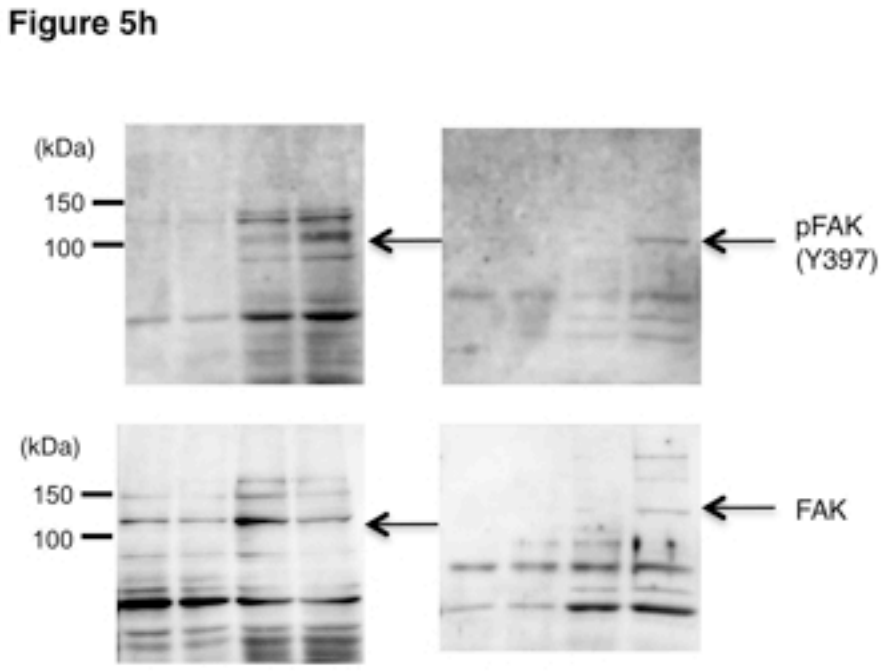

Supplementary Figure S25 cont.

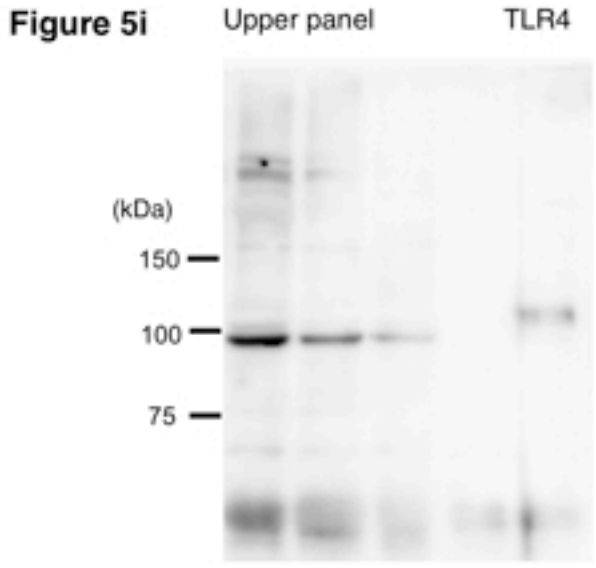

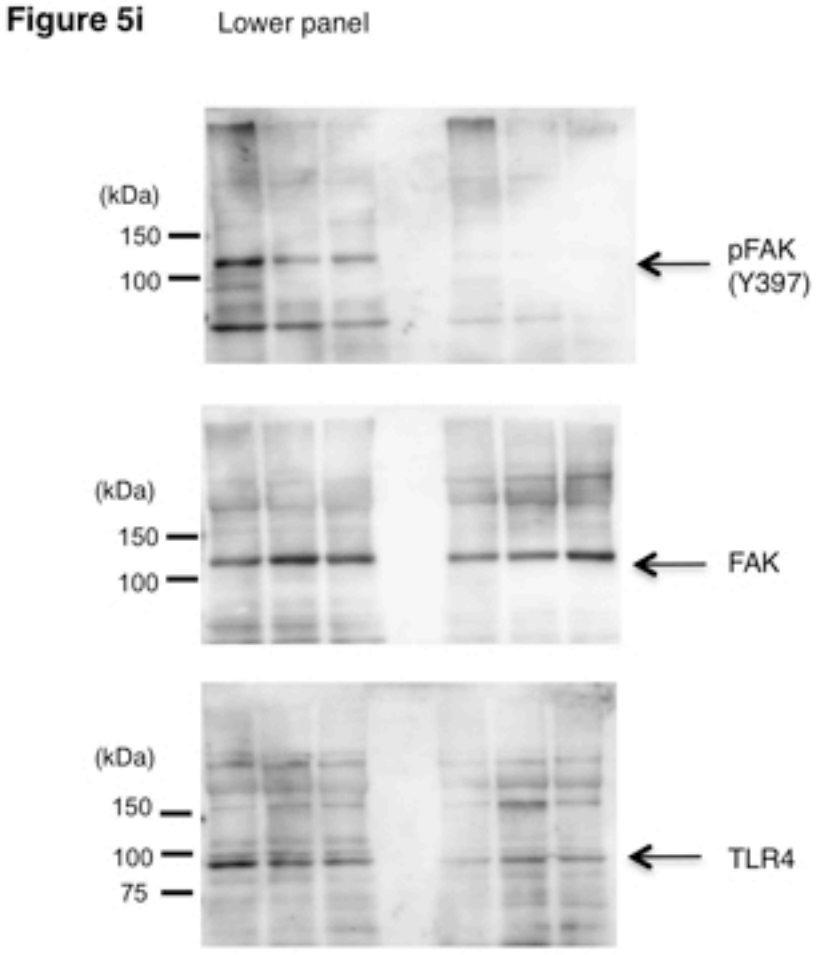

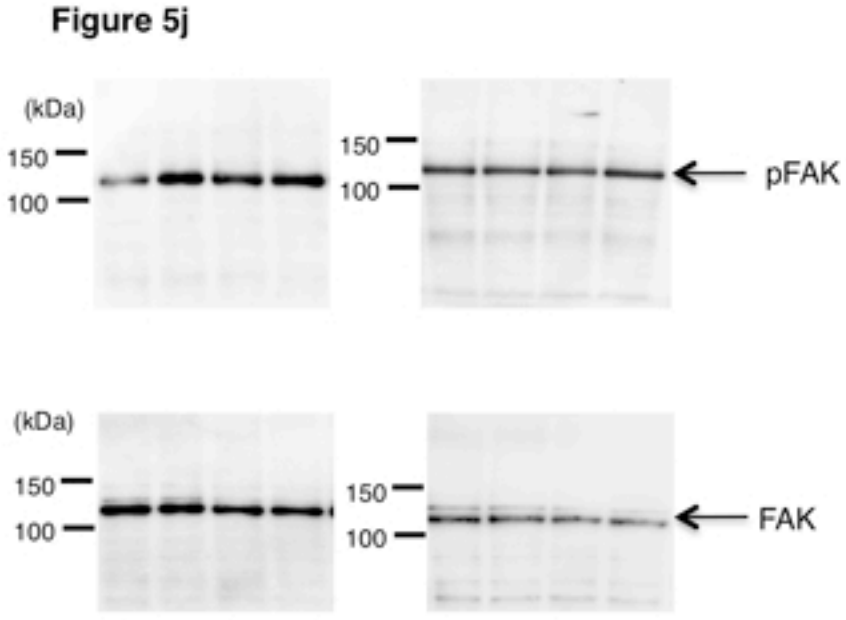

Supplementary Methods

Reagents

The tyrphostin AG490, SB202190, wortmannin, were purchased from Sigma. The anti-pJak2 (phosphoY1007+Y1008) Ab (ab32101) were from Abcam. The anti-pAkt (Ser473) Ab, anti-pP38 mitogen-activated protein kinase (MAPK) Ab, anti-p38 MAPK Ab, anti-Akt Ab, and anti-Jak2 (D2E12) Ab were from Cell Signaling

Miles vascular permeability assay Potential stimulators of vascular permeability were intradermally injected into the flanks of C57BL/6 mice before the i.v. injection of EB dye in saline.

Quantitative-PCR

The following primers were used for the PCR: β-actin, 5'-TTCTTTGCAGCTCCTTCGTT-3' and 5'-ATGGAGGGGAATACAGCCC-3'; CCR2, 5'-AACAGTGCCCAGTTTTCTATAGG-3' and 5'-CGAGACCTCTTGCTCCCCA-3'; CCL2, 5'-ATGCAGGTCCCTGTCATGCT-3' and 5'-CTAGTTCACTGTCACACTGG-3'; S100A8, 5'-CCGTCTTCAAGACATCGTTTGA-3' and 5'-GTAGAGGGCATGGTGATTTCCT-3'; S100A9, 5'-GTCCAGGTCCTCCATGATGT-3' and 5'- GAAGGAAGGACACCCTGACA -3'; SAA3, 5'-GTTGACAGCCAAAGATGGGT-3' and 5'-CCCGAGCATGGAAGTATTTG-3'; TNFα, 5'-ATGAGAGGGAGGCCATTTG-3' and 5'-CAGCCTCTTCTCATTCCTGC-5'; Fcgr2b, 5'-TCTTCCTTGAGCACCTGGAT-3' and 5'-CTCACGGACTTTGTGCCATA-3';

Gpr65 5’-TGCTTGCCCTTTTGAATCTT-3’

and 5’-AAGCATCCCTCCAGAAACAG-3’; Pira1

5’-CGAGAGCTTCTGTGGTCCTT-3’ and 5’-TACTGGACACCCAGCCTTTT-3’;

Csf3r 5’-AGCAAAGTATGCCCAGGAAA-3’ and

5’-ATGTCTACCTCATGGCCACC-3’; and Il1r2

5’-TGGTGAAAGCAGAAACTCCA-3’

and 5’-AGGCAAGAAGCAGCAAGGTA-3’.